Experiments and numerical simulation of a diode-laser-pumped Cr, Nd:YAG self-*Q*-switched laser

Jun Dong, Jianren Lu, and Ken-ichi Ueda

Institute for Laser Science, University of Electro-Communications, 1-5-1 Chofugaoka, Chofu, Tokyo 182-8585, Japan

Received February 21, 2004; revised manuscript received June 7, 2004; accepted July 19, 2004

The self-Q-switched laser performance of a diode-laser-pumped monolithic Cr^{4+}, Nd^{3+}:YAG planar–planar 5-mm-long resonator was studied experimentally and theoretically. The dynamic characteristics of the self-Q-switched Cr, Nd:YAG laser were studied by solution of coupled rate equations. The effects of the pump rate, the reflectivity of the output couplers, and the concentrations of saturable absorbers on the laser performance were investigated in detail. The numerical simulation of the Cr, Nd:YAG lasers was in good agreement with the experimental results. We could optimize the laser performance by varying the pump rate, the concentration of the Cr^{4+} ions in the saturable absorber, and the reflectivity of the output coupler. A typical self-*Q*-switched laser pulse output of 19 μJ, 3.5 ns wide (FWHM) at a repetition rate of 26 kHz, was obtained, yielding 5.4 kW of peak power.

OCIS codes: 140.3540, 140.3580, 160.3380.

1. INTRODUCTION

In recent years, Cr^{4+}-doped crystals have attracted a great deal of attention as passive *Q* switches.[1–8] Cr^{4+}- and Nd^{3+}-codoped YAG crystal is an important self-Q-switched laser material.[9–16] However, we are aware of no reports of the effects of the pump power, the concentration of the saturable-absorbing ions, and the reflectivity of the output coupler on the performance of monolithic Cr, Nd:YAG lasers. In this paper we describe the performance of a diode-laser-pumped monolithic Cr, Nd:YAG self-*Q*-switched laser. The average output power, the single-pulse energy, the pulse width, the peak power, and the repetition rate of the 1064-nm laser output have been measured as functions of the absorbed pump power. The coupled rate equations of a self-*Q*-switched laser were evaluated, and the numerical solutions of the rate equations agree with the experimental results in the entire pump region. The effects of the pump rate, the reflectivity of the output coupler, and the concentration of the saturable-absorbing ions on the performance of Cr, Nd:YAG monolithic lasers were investigated in detail. A proposed optimized laser pulse output is described, as well as its achievement based on the experimental setup and on the numerical simulations detailed below.

2. EXPERIMENTS AND METHODS

The Cr, Nd:YAG crystal used in the experiment was grown by the standard Czochralski method. Cr^{4+} was substituted into a distorted tetrahedral Al site;[17] therefore a charge compensator was required, and $CaCO_3$ was added for that purpose. The nominal concentrations of Cr and Nd in the Cr, Nd:YAG crystal were 0.01 and 1 at. %, respectively. The absorption spectra were measured with a Cary 500 Scan UV-Vis-NIR spectrophotometer at room temperature. The resolution was set to be 0.1 nm. We estimated the ground-state absorption cross section of Cr, Nd:YAG by measuring the absorption coefficient of Cr^{4+} ions centered at 1064 nm and the concentration of Cr^{4+} in the Cr, Nd:YAG crystal. The saturation transmission was measured by use of a 1064-nm Nd:YAG pulse laser as the pump source; the pulse width was 5 ns. We recorded the transmission of Cr, Nd:YAG at different input pump energies by varying the focusing diameter of the pump source. We used the transmission data to determine the excited-state absorption cross section.

A schematic of the diode-laser-pumped Cr, Nd:YAG self-*Q*-switching laser cavity is shown in Fig. 1. A Cr, Nd:YAG crystal was polished to a plane–plane geometry as a laser resonator. The planar rear surface was coated for high transmission at 808 nm and total reflection at 1064 nm. The planar front surface, which served as the output coupler, was coated for 97% reflection at 1064 nm and total reflection at 808 nm. The overall cavity length was 5 mm. The misalignment of the axes of the two mirrors was measured to be less than 0.3°. A 1-W high-brightness Hamamatsu 2901 diode laser with a 50 μm $\times$ 1 μm emission cross section was used as the pump source. Owing to the large emission angles of the diode laser, the coupled optics (two focal lenses with a focal length of 8 mm) was used to focus the pump beam onto the crystal's rear surface. After the coupling optics, the pump light spot in Cr, Nd:YAG was ~150 μm in diameter. The laser operation was performed at room temperature. The *Q*-switched pulses were recorded with a fast Si P–I–N detector of 1.5-ns rise time and a Tektronix TDS 380 digitizing oscilloscope of 500-MHz sampling rate in the single-shot mode. The output power was measured with a laser powermeter. The laser's output beam profile near the output coupler was monitored with a CCD camera; we could estimate the beam diameter.

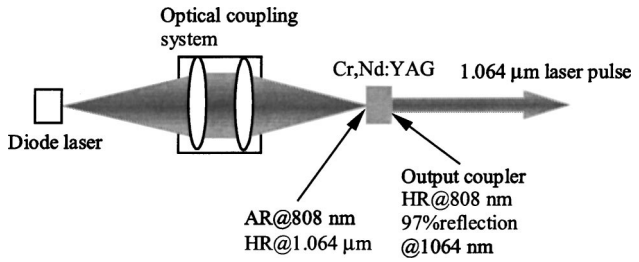

Fig. 1. Experimental setup of the self-Q-switching diode-laser-pumped Cr, Nd:YAG laser: AR, antireflective; HR, highly reflective.

The pulse energy was determined from the average output power and pulse repetition rate. The peak power was determined from the pulse energy and pulse width.

3. THEORETICAL MODEL

The coupled rate equations for the photon density and the population inversion density of the gain and the saturable-absorber medium in the self-Q-switching resonator, including the excited-state absorption of the saturable absorber and the population reduction factor of the laser, are as follows[18–20]:

$$\frac{\mathrm{d}\phi}{\mathrm{d}t} = \frac{\phi}{t_r}\left[2\sigma N l - 2\sigma_g N_g l - 2\sigma_e N_e l - \ln\left(\frac{1}{R}\right) - L\right], \tag{1}$$

$$\frac{\mathrm{d}N}{\mathrm{d}t} = -\gamma c\sigma\phi N - \frac{N}{\tau} + W_p, \tag{2}$$

$$\frac{\mathrm{d}N_g}{\mathrm{d}t} = -\sigma_g c\phi N_g + \frac{N_{s0} - N_g}{\tau_s}, \tag{3}$$

$$N_g + N_e = N_{s0}. \tag{4}$$

The notation used in Eqs. (1)–(4) is summarized in Appendix A. The absorption length of the Cr^{4+}-ion saturable absorber is the crystal length, l, for a monolithic Cr, Nd:YAG self-Q-switched laser. $\gamma = 1$ for Nd-doped solid-state lasers. Volume pump rate W_p is proportional to the cw pump power.

From Eq. (1), the loss of the Q-switched laser can be expressed as

$$\text{Loss} = \frac{2\sigma_g N_g l + 2\sigma_e N_e l + \ln(1/R) + L}{2\sigma l}. \tag{5}$$

The dynamic and laser characteristics of the passively Q-switched laser can be obtained by numerical solution of coupled rate equations (1)–(4) by use of Matlab 6.0 software.

Output pulse energy E, peak power P, and pulse width τ_p of the self-Q-switched Cr, Nd:YAG laser can be written as[19]

$$E = \frac{h\nu A l'}{t_r}\ln\left(\frac{1}{R}\right)\int_0^\infty \phi(t)\mathrm{d}t, \tag{6}$$

$$P = \frac{h\nu A l'}{t_r}\ln\left(\frac{1}{R}\right)\phi_{\max}, \tag{7}$$

$$\tau_p \approx E/P, \tag{8}$$

where $\int_0^\infty \phi(t)\mathrm{d}t$ is the integral of the cavity photon density over a temporal range covering the entire laser pulse and $\phi_{\max}$ is the maximum photon density in the laser cavity.

4. RESULTS AND DISCUSSION

The room-temperature absorption spectrum is shown in Fig. 2. Cr^{3+} is the dominant state in Cr-doped YAG crystal; Cr^{4+} can be formed by addition of Ca^{2+} ions for charge compensation while the crystal is grown or annealed in an O_2 atmosphere. However, Cr^{4+} is only a small fraction [~4% (Ref. 21)] of the total Cr-ion concentration added to the Cr, Nd:YAG crystal. The absorption spectrum of Nd^{3+} is superimposed over that of Cr^{3+}. The absorption spectrum of Nd^{3+} near 808 nm is shown in inset (a) of Fig. 2. There is a broad absorption spectrum of Cr^{4+} centered at 1064 nm, and the detailed absorption spectrum of Cr^{4+} centered about 1046 nm is shown in inset (b) of Fig. 2. The absorption coefficient is 7.3 cm^{-1} at a pumping wavelength of 808 nm for Nd^{3+} ions and is 0.2 cm^{-1} at 1064 nm for Cr^{4+} ions. The emission cross section is $2.35 \times 10^{-19}\,cm^2$ at 1064 nm with a lifetime of ~210 μs,[15] which is marginally shorter than that in Nd:YAG (230 μs). It is difficult to determine the spectroscopic parameters of Cr^{4+}:YAG crystal because of the presence of Cr^{3+} ions in the YAG host, the effect of the O_2 growth atmosphere, and the amount of charge-compensating ions such as Ca^{2+} and Mg^{2+}. Reported ground-state and excited-state absorption cross sections vary by an order of magnitude.[6–8] From our measurement of the absorption coefficient of Cr^{4+} at 1064 nm and from its estimated concentration in the Cr, Nd:YAG crystal, we calculated the ground-state absorption cross section to be $4.3 \times 10^{-18}\,cm^2$, which is in the range of reported values.[6–8] We determined the excited-state absorption cross section at 1064 nm by measuring the

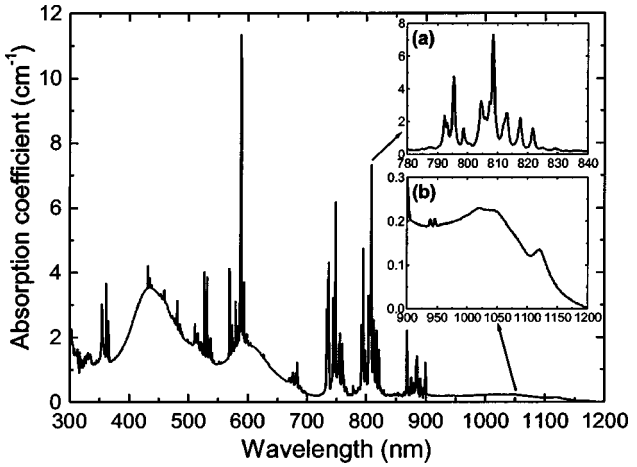

Fig. 2. Absorption spectrum of a Cr, Nd:YAG crystal at room temperature. (a) Absorption spectrum near 808 nm for Nd^{3+}, which is suitable for commercially available diode laser pumping; (b) absorption spectrum of Cr^{4+} centered at 1064 nm.

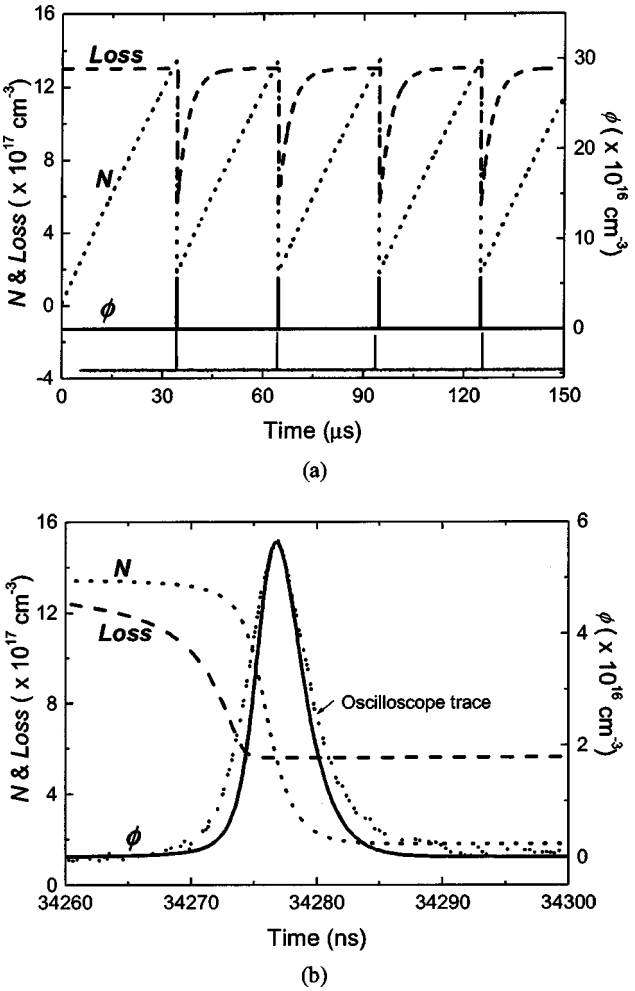

Fig. 3. Details of numerical calculations and experimental oscilloscope traces of the diode-laser-pumped Cr, Nd:YAG laser pulse train and a single pulse development in time. (a) Evolution of the photon density, gain inversion density, and loss on a time scale of the pulse repetition period. The measured oscilloscope pulse train is in arbitrary units for comparison with the numerical calculations. (b) Evolution of the photon density, gain inversion density and the loss on a time scale of the pulse width. In (a), the thin solid line is the experimental oscilloscope trace of the laser pulses; the thick lines are the numerical results. A pump rate of $W_p = 4 \times 10^{22}\,\mathrm{s}^{-1}\,\mathrm{cm}^{-3}$ was used for both figures. The measured oscilloscope trace was normalized at peak power for comparison with the numerical calculation.

saturation transmission curve of the sample, using the 1064-nm laser as the pumping source, to be $8.2 \times 10^{-19}\,\mathrm{cm}^2$, which is also in good agreement with the reported values.[8]

With Cr, Nd:YAG crystal as the active medium, by cw pumping, a repetitively Q-switched laser was obtained. The output laser pulse train was stable, and the variation of the pulse amplitude was within 10%. The thin solid line at the bottom of Fig. 3(a) shows the oscilloscope pulse train for 850 mW of absorbed pump power. The output laser was nearly TEM_{00} mode, and the laser beam's radius near the output coupler was estimated to be $\sim 85\ \mu\mathrm{m}$. The highest average output power of 102 mW at 1064 nm was obtained at an absorbed pump power of 850 mW. Each pulse had an energy of 3.3 μJ and a width of 5 ns, resulting in a peak power of 680 W at a repetition rate of 32 kHz. The short-dashed curve in Fig. 3(b) shows the oscilloscope pulse profile at 850 mW of absorbed pump power. The filled circles in Figs. 4(a), 4(b), 4(c), 4(d), and 4(e) show the pulse energy, the pulse width (FWHM), the repetition rate, the average output power, and the peak power, respectively, of a Cr, Nd:YAG self-Q-switched laser as functions of the pump rate. Pump rate W_p is proportional to the absorbed pump power and is given by the expression $W_p = P_{\mathrm{abs}}/h\nu_p A_p l$, where $P_{\mathrm{abs}} = P[1 - \exp(-2\alpha l)]$ for a two-pass pumping geometry, P is the pump power incident upon the crystal surface, $h\nu_p$ is the pump photon energy, A_p is the pump beam area at the entrance of the Cr, Nd:YAG crystal, and l is the crystal's length. It is assumed that the pump beam area inside the crystal changes little along the pump axis for the short cavity used. It can be seen that the average output power depends linearly on the pump rate and exhibits no saturation in the pump power range used. Thus much higher laser output power could be obtained by use of higher-power diode lasers as the pump source. The threshold pump power was approximately 250 mW, and the slope efficiency was 19.6%. The optical efficiency (the ratio of average output power to the absorbed pump power) of the self-Q-switched laser was approximately 12%. The pulse's repetition rate and width are also influenced by the absorbed pump power. Repetition rate f increases linearly with the absorbed pump power, as expected from the theory. The pulse width narrows considerably with the absorbed pump power at low pump rates and continues to narrow moderately at higher pump rates.

Figure 3 shows the results of the numerical simulation for the self-Q-switched Cr, Nd:YAG lasers obtained by solution of Eqs. (1)–(4) by the Runge–Kutta method for pump rate $W_p = 4 \times 10^{22}\,\mathrm{s}^{-1}\,\mathrm{cm}^{-3}$, which corresponds to an absorbed pump power of 850 mW. The other parameters used in this simulation are listed in Appendix B. It takes $\sim 34\ \mu$s to develop the first Q-switched laser pulse; the time interval between subsequent Q-switched laser pulses is $\sim 30\ \mu$s, which is shorter than the time required for developing the first laser pulse because inversion density N does not decrease to zero after the release of the first laser pulse [Fig. 3(a)]. The repetition rate can be estimated as ~ 33 kHz, in a good agreement with experimental data [thin solid line at the bottom of Fig. 3(a)]. The thick curves in Fig. 3(b) are an expanded view of Fig. 3(a) near the occurrence of the first laser pulse. When the photon density inside the laser cavity increases, the loss decreases accordingly as a result of bleaching of the Cr^{4+}:YAG saturable absorber. The photon density reaches its peak value when the laser inversion population equals the cavity loss, i.e., when $N = \mathrm{Loss} = 5.6 \times 10^{17}\,\mathrm{cm}^{-3}$. Beyond this point the laser inversion density (gain) is smaller than the total loss of the laser system, and the Q-switched laser pulse dies out quickly while the laser inversion density decreases gradually to a minimum value of $\sim 1.8 \times 10^{17}\,\mathrm{cm}^{-3}$. The increase in the loss after the release of the Q-switched laser pulse is due to relaxation of the population of Cr^{4+} saturable-absorber ions. In Fig. 3(b) the calculated pulse profile is in good agreement with that of the experiment (short-dashed curve). The measured oscilloscope trace was nor-

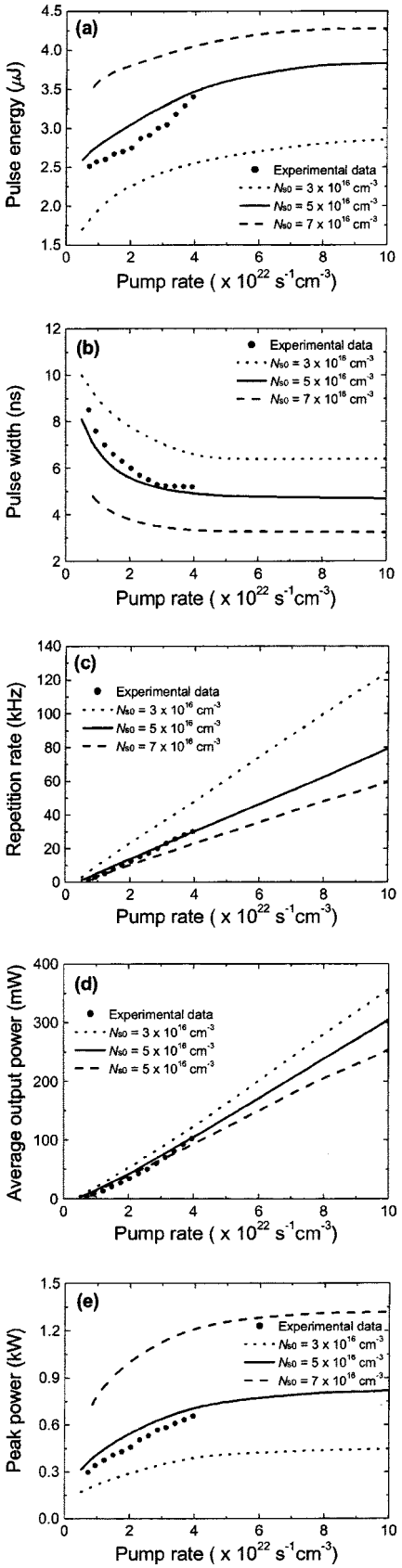

Fig. 4. Diode-laser-pumped Cr, Nd:YAG self-Q-switched laser output characteristics (a) pulse energy, (b) pulse width, (c) repetition rate, (d) average output power, and (e) peak power as functions of pump rate for three Cr^{4+}-ion concentrations of the saturable absorber.

malized for comparison with that of our numerical calculation. The pulse width (full width at half-maximum) was ~4.5 ns, which is a bit shorter than the measured laser pulse width (5 ns). We consider this difference to be the result of defects inside the crystal and of a transverse variation in the pump beam that was not included in the numerical model. The computed output pulse energy was ~3.5 μJ, and the peak power was ~780 W.

Obviously, the cw pump power strongly affects all the performance parameters of a Q-switched laser. The average output power increases with the absorbed pump power. The curves in Fig. 4 show the self-Q-switched laser's pulse energy, pulse width, repetition rate, average output power, and peak power as functions of pump rate W_p at 1064 nm for 97% reflectivity of the output coupler and various concentrations N_{s0} of the Cr^{4+} saturable absorbers. The Q-switched laser pulse energy increases with the pump rate for various concentrations of Cr^{4+} ions in a range from 3×10^{16} to $7 \times 10^{16}\,\mathrm{cm}^{-3}$ (the length of the saturable absorber remains constant). The pulse energy increases with the concentration of Cr^{4+} ions in the same range [Fig. 4(a)]. The pulse width decreases with the pump rate for the same concentrations of the Cr^{4+}-ion saturable absorbers as well as with the concentration of the Cr^{4+} saturable-absorbing ions [Fig. 4(b)]. Near the pump power threshold, the pulse energy increases and the pulse width decreases sharply with increasing pump rate. After the pump rate reaches a value of approximately $3 \times 10^{22}\,\mathrm{s}^{-1}\,\mathrm{cm}^{-3}$, the increase in pulse energy and the decrease in pulse width diminish with increasing pump rate. It is obvious that improved Q-switched laser performance can be achieved by use of a high pump rate and a high concentration of Cr^{4+} ions, as expected from theory and demonstrated by the numerical simulations. Figure 4(c) shows the repetition rate as a function of the pump rate for three concentrations of the saturable-absorber Cr^{4+} ions. The repetition rate of Q-switched lasers increases linearly with the pump rate and decreases with the concentration of the saturable-absorber Cr^{4+} ions. Figure 4(d) shows the calculated average pump power as a function of the pump rate for three concentrations of Cr^{4+} ions. The average output power increases linearly with the pump rate, yet decreases with the concentration of Cr^{4+} ions; the cause may be the increase in the cavity loss owing to excited-state absorption by the saturable-absorber Cr^{4+} ions. The peak power increases with the pump rate as well as with the concentration of Cr^{4+} ions in the saturable absorber [Fig. 4(e)]. The peak power increases steeply with the pump rate at low pump rates and then slowly for pump rates greater than $3 \times 10^{22}\,\mathrm{s}^{-1}\,\mathrm{cm}^{-3}$.

Thus, good agreement was achieved between the experimental data and the numerical calculations. The average output power and repetition rate of the diode-laser-pumped Cr, Nd:YAG laser are in fair agreement with the numerical calculations for a saturable-absorber concentration of $5 \times 10^{16}\,Cr^{4+}\,\mathrm{ions/cm}^3$.

The reflectivity of the output coupler also has an effect on the Cr, Nd:YAG self-Q-switched laser characteristics. Figure 5 shows the pulse energy, the pulse width, the repetition rate, the average output power, and the peak power as functions of reflectivity of the output coupler for

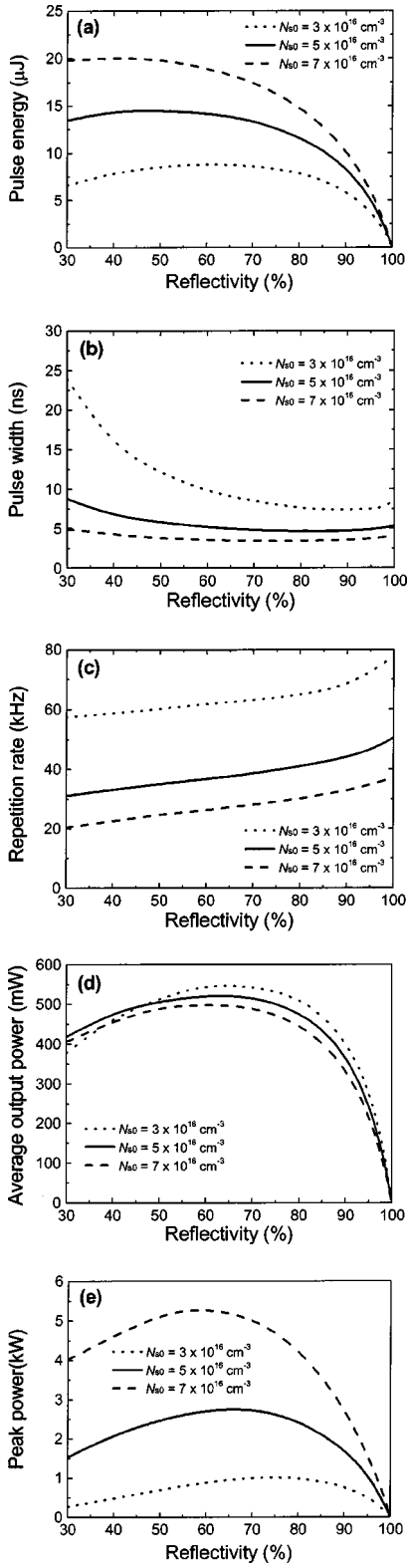

Fig. 5. Laser characteristics (a) pulse energy, (b) pulse width, (c) repetition rate, (d) average output power, and (e) peak power as functions of reflectivity of the output coupler for three concentrations of the Cr^{4+} saturable absorber. Pump rate, $6 \times 10^{22}\,s^{-1}\,cm^{-3}$.

three concentrations of saturable-absorber Cr^{4+} ions. A pump rate of $W_p = 6 \times 10^{22}\,s^{-1}\,cm^{-3}$ was used in these numerical calculations, and the other parameters remained unchanged and are listed in Appendix 2. The Q-switched pulse energy increases and the pulse width decreases with the concentration of Cr^{4+} ions for a specific reflectivity of the output coupler. The repetition rate of the Q-switched pulse decreases with increasing concentration of the saturable-absorber Cr^{4+}-ions. The results show that one can obtain a better self-Q-switched Cr, Nd:YAG laser performance, in terms of a narrow pulse width and a high pulse energy output, by increasing the concentration of saturable-absorber Cr^{3+} ions. From Fig. 5(a), the Q-switched pulse energy decreases steeply with the reflectivity of the output coupler, especially when the reflectivity becomes close to unity. The pulse energy increases with the concentration of saturable-absorber Cr^{4+} ions. The pulse energy decreases slowly when the reflectivity of the output coupler ranges from 40% to 70% for a constant concentration of saturable-absorber Cr^{4+} ions. As indicated in Fig. 5(b), there is an optimum reflectivity of the output coupler for which the shortest pulse width of self-Q-switched Cr, Nd:YAG laser can be achieved. The optimum reflectivities of output couplers are approximately 80%, 82%, and 90% for Cr^{4+}-ion concentrations of 7×10^{16}, 5×10^{16}, and $3 \times 10^{16}\,cm^{-3}$, respectively. The pulse width increases steeply with the reflectivity of the output coupler when the reflectivity of the output coupler is close to unity. The Q-switched pulse repetition rate increases with the reflectivity of the output coupler and decreases with the concentration of saturable-absorbing Cr^{4+} ions for a constant reflectivity (such as 90% reflectivity) of the output coupler [Fig. 5(c)]. The average output power increases with decreasing output coupling for the three concentrations (3×10^{16}, 5×10^{16}, and $7 \times 10^{16}\,cm^{-3}$) of saturable absorbers, and there are optimum reflectivities of 65%, 62%, and 60%, respectively, for obtaining the highest average output power [Fig. 5(d)]. There is a slightly decrease of the average output power with increasing concentrations of the saturable-absorber Cr^{4+} ions; this was probably caused by the increase in the concentration of the saturable-absorber Cr^{4+} ions that brought about an increase in the cavity loss. From Figs. 5(a) and 5(b), parameters for the best self-Q-switched Cr, Nd:YAG laser performance in terms of higher peak power can be obtained. The reflectivities of the output coupler to achieve the highest peak power output should be near 80%, 70%, and 60%, respectively, for three concentrations of saturable-absorber Cr^{4+} ions {3×10^{16}, 5×10^{16}, and $7 \times 10^{16}\,cm^{-3}$ [Fig. 5(e)]}.

One can improve the performance of the self-Q-switched Cr, Nd:YAG laser by optimizing various parameters, such as by using a high pump rate and a high Cr^{4+}-ion saturable-absorber concentration, and by suitable reflectivity of the output coupler. Based on the current monolithic Cr, Nd:YAG self-Q-switched laser experimental configuration, a Q-switched laser pulse of 19 μJ with a pulse width of 3.5 ns can be obtained for a laser cavity 5 mm long with 60% reflectivity of the output coupler, a concentration of the saturable absorber of $N_{s0} = 7 \times 10^{16}\,cm^{-3}$, and a $6 \times 10^{22}\,s^{-1}\,cm^{-3}$ pump rate. The repetition rate of such a laser system is 26 kHz, and the peak power will be ~5.4 kW. By varying the parameters in the simulations, one may predict the output laser

characteristics. This is important for the development of diode-laser-pumped Cr, Nd:YAG *Q*-switched lasers used in various applications such as remote ranging and pollution monitoring.

5. CONCLUSIONS

We have investigated the dynamic and laser characteristics of a self-*Q*-switched Cr, Nd:YAG laser by numerically solving the relevant rate equations. The modified coupled rate equations include the pump rate term, and the excited-state absorption of the saturable absorber was solved numerically. The laser characteristics were studied in detail as functions of the initial population of the ground state of the Cr^{4+} saturable-absorber ions, the pump rate, and the reflectivity of the output coupler. The simulation results show that the results obtained numerically are in good agreement with those obtained experimentally. Optimized laser performance can be achieved by use of a high-concentration Cr^{4+}-ion saturable absorber, a high pump rate, and the optimum reflectivity of the output coupler for a specific concentration of Cr^{4+}-ion saturable absorber. A typical self-*Q*-switched 19-μJ laser pulse, 3.5 ns wide and with 5.4-kW peak power at a 26-kHz repetition rate, can be achieved.

APPENDIX A. NOTATION USED IN THE RATE EQUATIONS

Parameter	Description
ϕ	Photon density in the laser cavity
l'	Optical length of the laser cavity
N	Population inversion density of the laser rode
σ	Stimulated emission cross section of the laser crystal
$t_r = 2l'/c = 2nl/c$	Cavity round-trip time
n	Refractive index of the laser crystal
l	Length of the laser crystal
c	Vacuum speed of light
σ_g	Ground-state absorption cross section of the saturable absorber
σ_e	Excited-state absorption cross section of the saturable absorber
N_g	Ground-state population density of the saturable absorber
N_e	Excited-state population density of the saturable absorber
N_{s0}	Total population density of the saturable absorber
R	Reflectivity of the output coupler
L	Nonsaturable intracavity round-trip dissipative optical loss
γ	Inversion reduction factor
W_p	Volume pump rate into the upper laser level
τ	Lifetime of the upper laser level of the gain medium
τ_s	Excited-state lifetime of the saturable absorber
A	Active area of the beam in the laser medium
$h\nu$	Laser photon energy

APPENDIX B. PARAMETERS USED IN THE NUMERICAL SIMULATIONS

Constant	Value	Reference
σ (cm^2)	2.35×10^{-19}	15
σ_g (cm^2)	4.3×10^{-18}	6–8
σ_e (cm^2)	8.2×10^{-19}	8
τ (μs)	210	15
τ_s (μs)	3.4	8
γ	1	
$h\nu_p$ (J)	2.46×10^{-19}	
$h\nu$ (J)	1.87×10^{-19}	
R (%)	97	
L	0.06	
A (cm^2)	2.3×10^{-4}	
N_{s0} (cm^{-3})	5×10^{16}	
l (mm)	5	
λ_p (nm)	808	
λ (nm)	1064	

ACKNOWLEDGMENTS

This research was supported by the 21st Century Center of Excellence program of the Ministry of Education, Science and Culture of Japan.

J. Dong's e-mail address is jundong_99@yahoo.com.

REFERENCES

1. P. Yankov, "Cr^{4+}:YAG *Q*-switching of Nd:host laser oscillators," J. Phys. D **27**, 1118–1120 (1994).
2. Y. Shimony, Z. Burshtein, and Y. Kalisky, "Cr^{4+}:YAG as passive *Q*-switch and Brewster plate in a Nd:YAG laser," IEEE J. Quantum Electron. **31**, 1738–1741 (1995).
3. K. Spariosu, W. Chen, R. Stultz, and M. Birnbaum, "Dual *Q*-switching and laser action at 1.06 and 1.44 μm in a Nd^{3+}:YAG-Cr^{4+}:YAG oscillator at 300 K," Opt. Lett. **18**, 814–816 (1993).
4. J. J. Zayhowski and C. Dill, "Diode-pumped passively *Q*-switched picosecond microchip lasers," Opt. Lett. **19**, 1427–1429 (1994).
5. Y. Shimony, Z. Burshtein, A. Ben-Amar, Y. Kalisky, and M. Strauss, "Repetitive *Q*-switching of a cw Nd:YAG laser using a Cr^{4+}:YAG saturable absorber," IEEE J. Quantum Electron. **32**, 305–310 (1996).
6. B. Lipavsky, Y. Kalisky, Z. Burshtein, Y. Shimony, and S. Rotman, "Some optical properties of Cr^{4+}-doped crystals," Opt. Mater. (Amsterdam, Neth.) **13**, 117–127 (1999).
7. G. Xiao, J. H. Lim, S. Yang, E. Van Stryland, M. Bass, and L. Weichman, "Z-scan measurement of the ground and excited state absorption cross sections of Cr^{4+} in yttrium aluminum garnet," IEEE J. Quantum Electron. **35**, 1086–1091 (1999).
8. Z. Burshtein, P. Blau, Y. Kalisky, Y. Shimony, and M. R. Kokta, "Excited-state absorption studies of Cr^{4+} ions in several garnet host crystals," IEEE J. Quantum Electron. **34**, 292–299 (1998).
9. S. Zhou, K. K. Lee, and Y. C. Chen, "Monolithic self-*Q*-switched Cr, Nd:YAG laser," Opt. Lett. **18**, 511–512 (1993).
10. Y. C. Chen, S. Li, K. K. Lee, and S. Zhou, "Self-stabilized single-longitudinal-mode operation in a self-*Q*-switched Cr, Nd:YAG laser," Opt. Lett. **18**, 1418–1419 (1993).

11. S. Li, S. Zhou, P. Wang, and Y. C. Chen, "Self-*Q*-switched diode-end-pumped Cr, Nd:YAG laser with polarized output," Opt. Lett. **18**, 203–205 (1993).
12. G. Yao, S. Zhou, P. Wang, K. K. Lee, and Y. C. Chen, "Dynamics of transverse mode in self-*Q*-switched solid-state lasers," Opt. Commun. **114**, 101–105 (1995).
13. P. Wang, S. Zhou, K. K. Lee, and Y. C. Chen, "Picosecond laser pulse generation in a monolithic self-*Q*-switched solid-state laser," Opt. Commun. **114**, 439–441 (1995).
14. J. Dong, P. Deng, Y. Lu, Y. Zhang, Y. Liu, J. Xu, and W. Chen, "Laser-diode-pumped Cr^{4+}, Nd^{3+}:YAG with self-*Q*-switched laser output of 1.4 W," Opt. Lett. **25**, 1101–1103 (2000).
15. J. Dong, P. Deng, and M. Bass, "Cr, Nd:YAG self-*Q*-switched laser with high efficiency output," Opt. Laser Technol. **34**, 589–594 (2002).
16. R. Feldman, Y. Shimony, and Z. Burshtein, "Passive *Q*-switching of Nd:YAG/Cr^{4+}:YAG monolithic microchip laser," Opt. Mater. (Amsterdam, Neth.) **24**, 393–399 (2003).
17. R. Feldman, Y. Shimony, and Z. Burshtein, "Dynamics of chromium ion valence transformation in Cr, Ca:YAG used as laser gain and passively *Q*-switching media," Opt. Mater. (Amsterdam, Neth.) **24**, 333–344 (2003).
18. W. Kochner, *Solid State Laser Engineering*, 3rd ed. (Springer-Verlag, Berlin, 1992), Chap. 8.
19. J. J. Degnan, "Optimization of passively *Q*-switched lasers," IEEE J. Quantum Electron. **31**, 1890–1901 (1995).
20. X. Zhang, S. Zhao, Q. Wang, Q. Zhang, L. Sun, and S. Zhang, "Optimization of Cr^{4+}-doped saturable-absorber *Q*-switched lasers," IEEE J. Quantum Electron. **33**, 2286–2294 (1997).
21. A. G. Okhrimchuk and A. V. Shestakov, "Performance of YAG:Cr^{4+} laser crystal," Opt. Mater. (Amsterdam, Neth.) **3**, 1–13 (1994).